Interaction between Photoactivated Rhodopsin and the C-Terminal Peptide of Transducin α-Subunit Studied by FTIR Spectroscopy[†]

Shoko Nishimura,[‡] Hideki Kandori,*[,‡] and Akio Maeda[‡,§]

Department of Biophysics, Graduate School of Science, Kyoto University, Sakyo-ku, Kyoto 606-8502, Japan, and Center for Biophysics and Computational Biology, University of Illinois, Urbana, Illinois 61801

Received June 18, 1998; Revised Manuscript Received August 25, 1998

ABSTRACT: Structural changes in the complex formed between photolyzed bovine rhodopsin and a synthetic 11-mer peptide corresponding to the C-terminal region of the transducin α-subunit (Gtα) were analyzed by means of Fourier transform infrared spectroscopy. A complex with a protonated Schiff base appears at the beginning, accompanying the formation of an α-helix. This complex evolves into another which abolishes the original structure but retains the protonated Schiff base. This complex exhibits the same spectral shape as that of the final stable complex with an unprotonated Schiff base. The Fourier transform infrared spectrum for the formation of this final complex was compared to that with transducin [Nishimura, S., Sasaki, J., Kandori, H., Matsuda, T., Fukada, Y., and Maeda, A. (1996) *Biochemistry 35*, 13267−13271]. A large part of the frequency shifts of the peptide carbonyl vibrations which form upon complex formation with transducin but are absent with the synthetic 11-mer peptide must be structural changes in other sites, such as the nucleotide binding site in Gtα. The peptide, like transducin, shows the perturbation of a carboxylic acid in an extremely apolar environment. Some of the changes in the peptide backbone remain in the complex formed with the peptide. These are due to sites where rhodopsin interacts with the C-terminal region of Gtα. Specifically, the labeling of the peptide amide corresponding to Leu349 of transducin by ^{15}N reveals weakening of the hydrogen bond of the peptide N−H of Leu349 and/or distortion of a peptide bond between Gly348 and Leu349 upon complex formation.

Heterotrimeric G proteins and G protein-coupled heptahelical receptors are widely present in various cellular signal transduction systems (*1*, *2*). Photoactivated rhodopsin and transducin (Gt)[1] are part of a visual transduction system. The guanine nucleotide exchange reaction in the α-subunit of Gt is catalyzed by metarhodopsin II (MII), one of the intermediates in the light-induced activation process of visual pigment rhodopsin; this is a crucial step for its liberation from the membrane-bound form. Gt is also virtually free from spontaneous activation without light. This enables us to induce the reaction in the mixture of rhodopsin and Gtα strictly light-dependent manner and to detect the structural changes with quite high fidelity by applying spectroscopic methods.

Two sites in the α-subunit of Gt (Gtα), one in the C-terminal region and the other close to it, have been identified as responsible for the binding of Gt to rhodopsin (*3*), using the corresponding synthetic peptides to compete with Gt for binding to MII. The residues 340−350[2] (IKENLKDCGLF) in the C-terminal region of Gtα exhibit stronger interaction with rhodopsin than the other peptide close to the C-terminus. It also stimulates the formation of MII in the absence of Gt, as the GDP-bound form of Gt does (*4*). The critical residues for the binding are further identified by use of either synthetic peptides (*5*) or recombinant Gtα (*6*, *7*) with replacements in specific residues. Leu344 and Leu349, which are conserved in α-subunits of various G proteins (*6*), are essential for the binding of Gtα to MII. Hydrophobic residues are always present at position 340, 344, 349, and 350 in the active peptides in a random peptide library (*5*). The interaction is absent in Gtα, whose Cys347 is ADP-ribosylated by pertussis toxin (*8*). The C-terminal region of the G protein α-subunit is generally important in determining the specificity of the receptor−G protein interaction (*9*). The crystallographic three-dimensional structure of Gtα, however, does not show clear structure for this C-terminal region (*10*−*13*). Different conformations of the C-terminal 11-mer peptide with and without the interaction with MII deduced by NMR spectroscopy (*14*) were later shown to contain errors (*15*). A different picture for these conformations was recently given by Kisselev et al. (*16*). Fourier transform infrared (FTIR) spectroscopy was used previously for the complex formation between MII and Gt. This technique is suitable to probe microenvironments of the specific protein bonds, the changes in hydrogen bonds (*17*). The changes upon complex formation in the hydrogen bonds of several peptide carbonyl

[†] This work is partially supported by grants from the Japanese Ministry of Education, Culture, Sports and Science to H.K. (09833002, 10129215, 10146228, 10358016).

* To whom all correspondence should be addressed. Phone and fax, 81-75-753-4210. E-mail, kandori@photo2.biophys.kyoto-u.ac.jp.

[‡] Kyoto University.

[§] University of Illinois.

[1] Abbreviations: Gt, transducin; MII, metarhodopsin II; Gtα, transducin α-subunit; FTIR, Fourier transform infrared; MI, metarhodopsin I; HOOP, hydrogen out-of-plane; Rh*, photolyzed rhodopsin capable of forming the complex with 11-mer peptide.

[2] Residue numbers in the C-terminal peptide were given according to the residue number in Gtα.

10.1021/bi981451n CCC: $15.00
Published on Web 10/20/1998

and amide groups were not attributable to a gross conformation change but to hydrogen bonding changes in one or a few peptide backbone groups (*18*). Such changes in the polar peptide backbone are important for function, as was detected in bacteriorhodopsin (*19*, *20*), rhodopsin (*21*), and the histocompatibility complex (*22*).

The changes due to complex formation could occur not only in a site for direct interaction but also in remote sites in rhodopsin and Gtα. Structural changes in the site for direct interaction should remain detectable in a spectrum upon complex formation with a synthetic peptide corresponding to a binding site of Gtα to rhodopsin. Also, the use of peptides depleted of other functional sites would give uncoupled events, which were recently detected at low temperature for detergent-solubilized rhodopsin with intact Gt (*23*, *24*). In the present study, we examined time-dependent structural changes in the complex formation of photoactivated rhodopsin with an 11-mer synthetic peptide in the C-terminal region of Gtα by means of conventional FTIR spectroscopy. Progressive structural changes in the complex were detected. We also aimed at resolving two problems regarding the final stable complex. One was to distinguish changes in the site for the direct interaction with the C-terminus of Gtα from those in other sites by comparing FTIR spectra for the complex formation with the peptide and Gt reported previously (*18*). The other was to search for possible structural changes of the peptide backbone at crucial two-leucine residues by ^{15}N labeling of each of their peptide amides.

MATERIALS AND METHODS

Rhodopsin in bovine rod outer segments was prepared as described previously (*25*). An 11-mer synthetic peptide at the C-terminus of Gtα with replacement of Lys341 by arginine (IRENLKDCGLF) was used (*14*). This analogue was shown to be the functional equivalent of the unsubstituted one, despite a recent criticism (*16*). This peptide and its derivative with a substitution of Leu349 by alanine (IRENLKDCGAF) were produced by Chiron Technologies Pty., Ltd., and purchased from Kurabo Industries Ltd.. The labeled peptides with ^{15}N at the peptide amide of Leu344 or Leu349 were also synthesized by replacing 9-fluorenylmethyloxycarbonyl leucine with its ^{15}N derivative purchased from Cambridge Isotope Laboratories Inc. (Andorn, MA). Final purification of the synthesized peptides by reverse-phase HPLC was carried out in a water−acetonitrile gradient system containing 0.1% trifluoroacetic acid. Each peak was identified by mass spectroscopy. Purity of the peptide samples examined by reverse-phase HPLC was more than 95%. Each weighed, lyophilized peptide was dissolved in buffer A composed of 10 mM MOPS buffer, pH 7.5, containing 100 mM NaCl, 2 mM $MgCl_2$, 1 mM DTT, and proteinase inhibitors (0.1 mM phenylmethylsulfonic acid, 4 μg/mL of aprotinin, and 4 μg/mL of leupeptin) so as to obtain a final concentration of 7 mM. The concentrations of the unlabeled and labeled peptides were then adjusted to the same concentration by adding buffer A on the basis of the concentration determined by a copper−Folin reagent color reaction method (*26*). The apparent concentration determined by this method was 66 ± 1% of the weighed values for all the samples, if one used human angiotensin I (a 10-mer peptide DRVYIHPFHL, molecular weight 1296.5), whose weight is calibrated in a range of 1% (purchased from Peptide Institute Inc., Minoh, Osaka, Japan), as a reference. The apparently smaller weight in the color reaction could arise from a less sensitive response of a cysteine residue in the 11-mer peptide in place of a tyrosine residue in angiotensin I. Nevertheless, we adopted the weighed value because the peptides were prepared so as to not contain any nonpeptide materials. The results of the color reaction ensures that the same weight was used for unlabeled and labeled peptides. The pH of the sample was adjusted to 7.5 ± 0.1 by use of a semiconductor-type pH electrode, pH BOY-P2 (SU-19).

Subsequent procedures for the preparation of the sample described below were done under dim red light. The peptide dissolved in buffer A was mixed with rhodopsin in a concentrated paste in buffer A. The mixture of 6.2 mM peptide and 6.0 μM rhodopsin was centrifuged at 90 000 rpm for 30 min at 4 °C in a TLA 100.3 rotor in a Beckman ultracentrifuge, model TL100. The final concentration in the precipitates of rhodopsin was estimated to be 2.3 mM from its visible spectrum. The concentration of the peptides in the pellet was estimated to be ∼2 mM by assuming that its amount was proportional to water content and determining the intensity of the O−H stretching vibration of water in the absolute FTIR spectrum of the pellet. The pellet thus obtained was kept at 0 °C in the dark before use. For each recording, about 0.5 μL of the pellet sample was transferred to a BaF_2 window and sandwiched by another BaF_2 window with a Teflon spacer 12.5 μm in thickness. The sample in a holder made of copper was mounted in an Oxford DN1704 cryostat in a BioRad FTS60A/896 for FTIR spectroscopy and a CF1204 cryostat in a Shimadzu spectrophotometer MPS-2000 for visible spectroscopy. Each cryostat was equipped with an Oxford ITC-4 temperature controller, and the temperature was regulated in a range of 0.1 K. Although the illumination pathways in both the FTIR and visible spectrometers are not constructed in the same way, the photoreactions proceeded in a very similar rate under these illumination conditions. Difference FTIR and visible spectra upon illumination for 10 s with light through a Toshiba Y-52 filter (a long-pass filter transmitting light above 500 nm with a half transmitting point at 520 nm) from a 1-kW halogen−tungsten lamp in a slide projector were obtained as reported previously (*18*). Each FTIR spectrum was constructed from 32 interferograms at a 2-cm^{-1} resolution. It takes 18 s for the recording. The spectra were corrected for the shape of the baseline by using the corresponding time-dependent spectra in the dark. All the difference spectra are displayed by scaling with the amount of photolyzed rhodopsin estimated from the intensity of a negative band at 970 cm^{-1} of the hydrogen out-of-plane (HOOP) mode due to the photolyzed rhodopsin. The recording of visible spectra gave a value at 380 nm at 52 s after the start of each scan.

RESULTS

Effect of the Peptide on MII Formation. It is known that illumination of rhodopsin in the membrane with >500 nm light for 10 s at 265 K yields a mixture of MII and its precursor, metarhodopsin I (MI) (*18*, *27*). The formation of MII after the illumination is monitored by the increase at 380 nm relative to the decrease at 570 nm due to photolyzed rhodopsin (Figure 1). The amount of MII attains a maximal

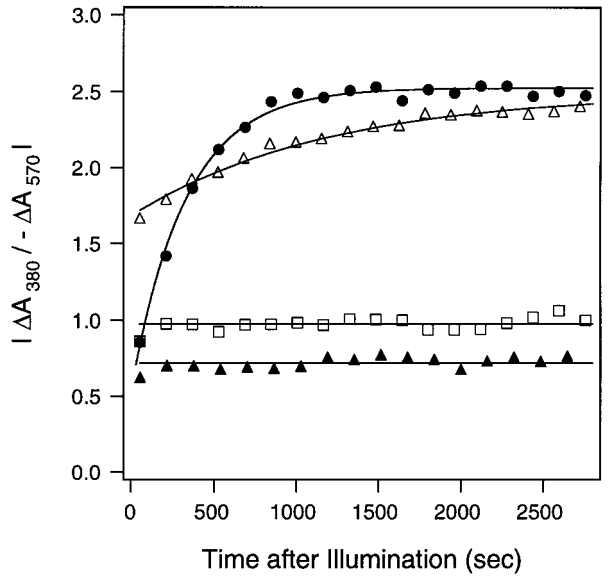

FIGURE 1: Formation of the MII−peptide complex. Changes in the total amount of MII, which were measured by the increase at 380 nm relative to the decrease at 570 nm due to photolyzed rhodopsin, are plotted against the time after illumination with >500 nm light for 10 s at 265 K. Closed circles and triangles show results in the presence of the unlabeled Gtα 11-mer peptide (residues 340−350 in Gtα) (IRENLKDCGLF) and its L349A analogue, respectively. The results in the presence of Gt and with only rhodopsin in a previous study (ref 18) are reproduced by open triangles and open squares, respectively.

level at 52 s after illumination in the first spectrum and stays at the same level up to 2800 s (open squares). In the presence of the K341R analogue of the 11-mer peptide (∼2 mM) from the C-terminal region of Gtα (IRENLKDCGLF) (closed circles), the amount of MII initially is almost the same as that in its absence. It then increases further with a $\tau_{1/e}$ of 330 s. To affirm that this peptide really works as an analogue of Gtα in the complex formation, we used an 11-mer peptide with alanine in place of Leu349 (IRENLKDCGAF) on the basis of a previous study which showed that an L349A mutant of Gtα is completely inactive for binding to MII (*6*). With the L349A peptide, the amount of MII stays at the same level throughout the incubation (closed triangles) as that attained at the beginning. The different levels in the absorbance ratios in the presence and absence of the L349A peptide are insignificant, because duplicate experiments on the unlabeled and labeled peptides exhibited similar differences in the final level, probably arising from an optical problem involving the sandwiched cell used in the present study. The reaction with Gt shows a final level similar to that with the peptide, though the process to it (open triangle, reproduced for comparison from ref 18) differs from that with the peptide.

FTIR Spectra in the Presence of the Peptide. The difference FTIR spectra in these processes are calculated by subtracting the spectra recorded just before the illumination from those at various times after illumination. The solid lines in Figure 2 show those recorded at 1360 s, when the reaction attains a steady level in the presence of the parent 11-mer peptide (a) and the L349A 11-mer peptide (b). These are compared with the spectra in the presence of Gt at 1360 s (c, reproduced from ref 18). Each spectrum is overlaid by a dotted line of the difference spectrum for rhodopsin only (in the absence of the peptides). Considerable changes

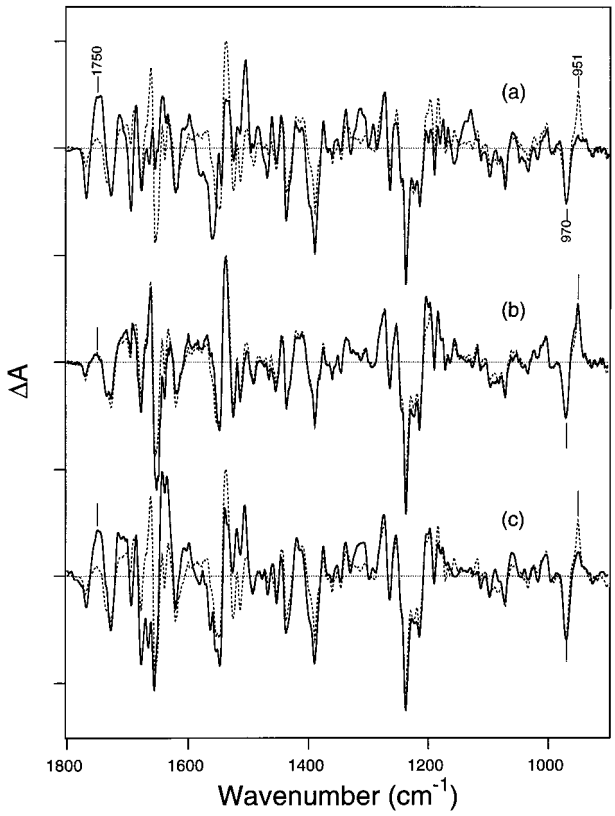

FIGURE 2: Difference FTIR spectra calculated from the spectra recorded before and 1360 s after illumination at 265 K. Dotted lines in a−c represent the results in the absence of the peptides duplicated from the previous paper (ref 18). Solid lines depict spectra in the presence of the parent 11-mer peptide (a), the L349A analogue peptide (b), and Gt (c, reproduced from ref 18). The spectra are the average of recordings with 20 (a), 8 (b), and 16 (c) fresh samples. The samples were illuminated under the same conditions as in Figure 1. One division of the ordinate corresponds to 0.001 absorbance unit.

appear when the parent peptide was added (solid line in a), whereas almost no changes are detected with the L349A peptide (solid line in b). The increase in the intensity of the 1750-cm^{-1} band upon addition of the parent peptide (solid line in a) is ascribable to the formation of the complex. This is accompanied by a parallel decrease in the intensity of the 951-cm^{-1} band of MI, indicating complex formation at the expense of MI. Spectral changes induced by Gt (solid line in c) are substantially different from those of the 11-mer peptide.

Time Course for Complex Formation. The ratio between MI and uncomplexed MII in the presence of the peptides must be the same as that in their absence because of an instantaneous equilibration between MI and MII in the photoproducts (*18*). Time-dependent changes in the content of the complex in the photoproducts in the presence of the 11-mer peptide (Figure 3, closed circles) were estimated from the changes in the ratio of the intensity of the 951-cm^{-1} band relative to that in the absence of the peptides. The points recorded at 40-s intervals are fitted with a single-exponential curve with $\tau_{1/e}$ of ∼100 s. A virtually identical time constant of 130 s was obtained by means of a singular value decomposition method (*28*) for the intensity changes in the 1800−1300 cm^{-1} region, where bands due to the peptide backbone and protonated carboxylic acids appear. Complex formation is also accompanied by the increase of the intensity

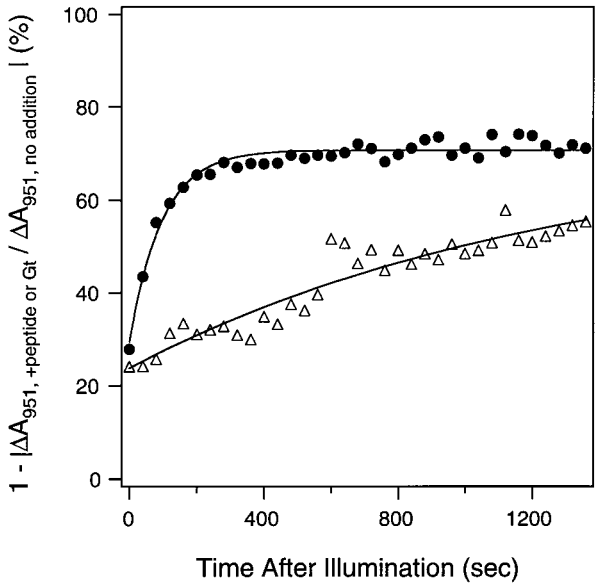

FIGURE 3: Time-dependent changes in the content of the complex in the photoproducts. Change in the ratio (%) of band intensity at 951 cm^{-1} in the presence of the parent peptide relative to that in the absence of the peptides was plotted against the duration after the offset of the illumination (closed circles). The results in the presence of Gt (open triangle) is also shown.

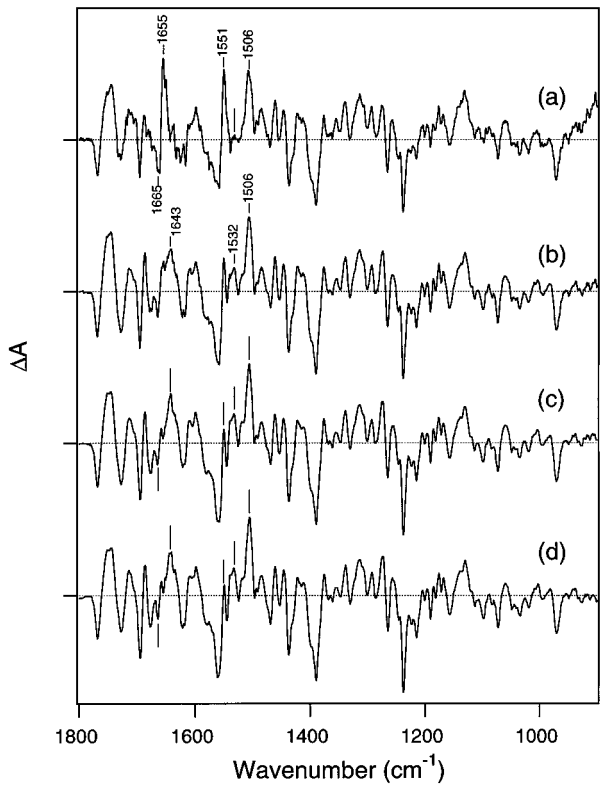

FIGURE 4: [Rhodopsin plus peptide → complex] spectra which were deduced from the spectra recorded just after the illumination (a) and at 120 s (b), 320 s (c), and 1360 s (d) after the illumination. One division of the ordinate corresponds to 0.002 absorbance unit.

at 1750 cm^{-1}. Time-dependent change in the amount of the complex, which was estimated as the ratio of increase in the intensity at 1750 cm^{-1} of each time point relative to that in the spectrum for the formation of MII (*18*), is virtually coincident with that attained by the intensity change at 951 cm^{-1} (not shown).

The process due to the complex formation occurs much faster than the peptide-dependent increase at 380 nm due to the deprotonation of the Schiff base ($\tau_{1/e}$ = ~330 s; Figure 1, closed circles). Thus, a species with the protonated Schiff base which is devoid of the 951-cm^{-1} band is present in the complex. However, from the fact that the final amount of the complex estimated from the intensity of the 951-cm^{-1} band, 71 ± 4% in the presence of the peptide at 1360 s, is almost the same as that estimated from the intensity increase at 1750-cm^{-1}, the 951-cm^{-1} band can be used to mark uncomplexed MI and the amount of the complex can be estimated from the decrease in the intensity at 951 cm^{-1}.

These results are in contrast to the case of the interaction of Gt with photoactivated rhodopsin; the $\tau_{1/e}$ value (1260 s) due to the decrease of the 951-cm^{-1} band of MI (Figure 3, open triangles) is nearly coincident with that (1180 s) estimated from the formation of MII in terms of increase at 380 nm (Figure 1, open triangles) (*18*). Because the same instruments were used for each FTIR and visible spectra in both the previous studies on Gt and the present studies on the peptides, this coincidence with Gt also ensures different $\tau_{1/e}$ values with the peptide. Nevertheless, the final amount of the complex in the presence of Gt (70 ± 5%), which was estimated from the fitted curve to the final level, is almost the same as for the peptide.

FTIR Spectrum for Complex Formation. The difference spectrum of [rhodopsin plus peptide → complex] is deduced for the spectrum at each time point by subtracting the contribution of the photoproducts which did not form the complex. This is obtained by multiplying the ratio of the intensity at 951 cm^{-1} in the presence and absence of the peptide (see closed circles in Figure 3) to the spectrum for rhodopsin only, as was done for the difference spectra of [rhodopsin plus Gt → complex] (*18*). The same series of spectra were recorded for 20 fresh samples and averaged for each time point. Figure 4 shows [rhodopsin plus peptide → complex] spectra at four typical time points. The first spectrum (a) shows the intense amide I and II bands at 1655 and 1551 cm^{-1} due to the α-helix in place of those at 1643 and 1532 cm^{-1} in the other spectra. This feature is largely lost in the second spectrum at 120 s (b). These results suggest the presence of two consecutively produced species with the protonated Schiff base before the formation of MII. The second spectrum (b) resembles the third spectrum at 320 s (c), which is identical with the fourth spectrum at 1360 s (d) due to the final stable complex. Thus, the spectrum of the second species with the protonated Schiff base is identical with that of the species with the unprotonated Schiff base. This is due to the fact that the vibrational modes of the chromophore do not contribute to these spectra. These spectra also differ from the [rhodopsin → MI] (*27*) and [rhodopsin → MII] spectra (*18*). Despite the contribution of the species with the protonated Schiff base, an average of all the spectra recorded at time points from 320 to 1360 s was expressed conventionally as the [rhodopsin plus peptide → Rh*−peptide complex] spectrum, where Rh* stands for the photolyzed rhodopsin which does not have the MI-specific 951-cm^{-1} band, and is shown in Figure 5a by a solid line. The previous study (*18*) shows that the shape of the difference spectrum for rhodopsin at 1360 s (dotted lines) is identical with that just after the illumination.

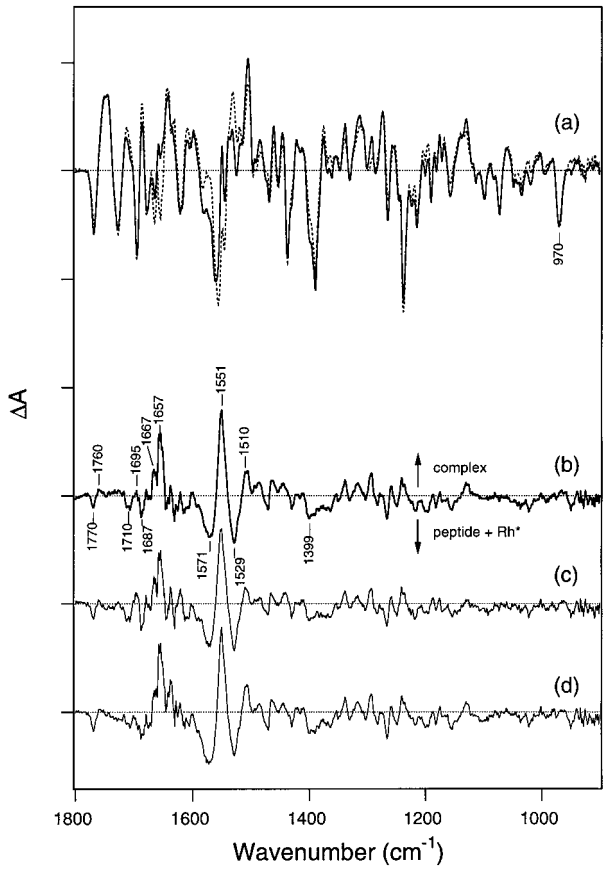

FIGURE 5: Difference FTIR spectra for the conversion from Rh* to the complex. The spectrum of [uncomplexed Rh* plus peptide → Rh*−peptide complex] (b) was calculated by subtracting the spectrum [rhodopsin → uncomplexed Rh*] (a, dotted line) from [rhodopsin plus peptide → Rh*−peptide complex] (a, solid line). The spectra shown by dotted and solid lines are scaled by the amount of photolyzed rhodopsin estimated from the intensity of a negative band at 970 cm^{-1}. The difference spectra in (c) and (d) are shown for duplicate data sets of 10 samples randomly divided from the 20 data sets. One division of the ordinate corresponds to 0.001 absorbance unit.

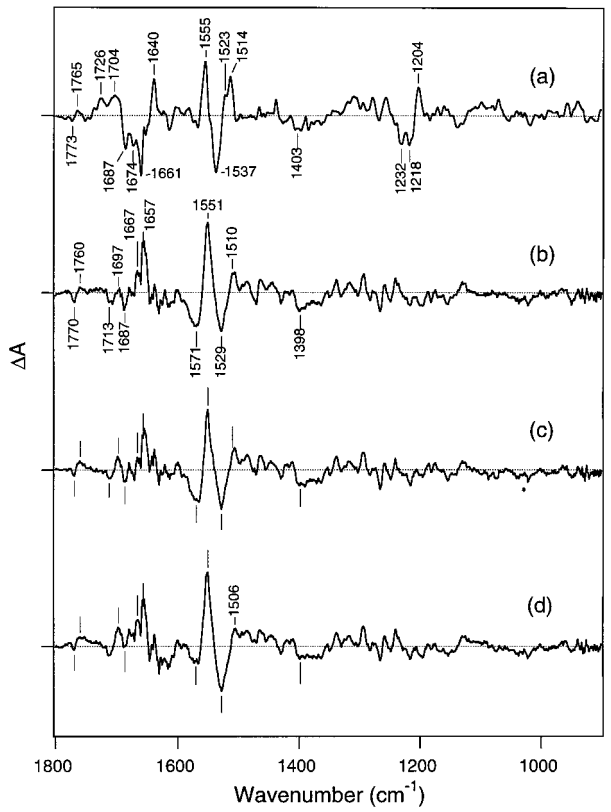

FIGURE 6: Difference FTIR spectra for the formation of the complex between Rh* and the parent peptide (b), the L344 ^{15}N-labeled peptide (c), the L349 ^{15}N-labeled peptide (d), and Gt (a, reproduced from ref 18). The spectra are scaled by the amount of photolyzed rhodopsin. One division of the ordinate corresponds to 0.002 absorbance unit.

Illumination with >500 nm light at 285 K gave a difference spectrum which does not show the 951-cm^{-1} band of MI (dotted line in Figure 5a), characteristic of MI which has no ability to interact with the peptide. This was used as a [rhodopsin → uncomplexed Rh*] spectrum. The subtraction of it from the [rhodopsin plus peptide → Rh*−peptide complex] spectrum (solid line) by scaling at the 970-cm^{-1} band yields the [Rh* plus peptide → Rh*−peptide complex] spectrum (Figure 5b). Two averaged difference spectra for each randomly divided 10 data sets derived from 20 data sets (Figure 5c and 5d) show nice reproducibility in both the frequency and the intensity of the bands.

Reactions with Rhodopsin and the 11-Mer Peptides. Having established the recording of the spectra with high reproducibility, we then compared the spectrum with the peptide (Figure 6b; duplicated from Figure 5b) to the spectrum for the formation of the Rh*−Gt complex (Figure 6a duplicated from ref 18).

A change of the bands at 1770 (−) and 1760 (+) cm^{-1} in the spectrum for the complex formation with the peptides (b) is ascribable to a protonated carboxylic acid residue from their frequencies, as are the bands at 1773 (−) and 1765 (+) cm^{-1} observed in the complex formation between Rh* and Gt (a). This may arise by the perturbation of the carboxylic acid in the peptide because the absolute spectrum of the 11-mer peptide exhibits a band around 1770 cm^{-1} (not shown), but we need further experiments with analogue peptides of either Glu342 or Asp346. Positive bands at 1726 and 1704 cm^{-1} in the Rh*−Gt complex formation (a), probably due to the protonation of the carboxylate, are not seen in the complex formation with the peptides. A change at 1403 cm^{-1}(−) in the Rh*−Gt complex formation (a) may be a corresponding unprotonated carboxylate.

Among frequency shifts of amide I bands at 1687, 1674, and 1661−1640 cm^{-1}, only the 1687-cm^{-1} band remains in the spectrum for the Rh*−peptide complex (b). Positive bands at 1667 and 1657 cm^{-1} in the Rh*−peptide complex formation (b) are not seen in the complex formation with Gt (a). This absence, however, could be due to cancellation by the intense negative bands around these frequencies.

Bands at 1232, 1218, and 1204 cm^{-1} (a) due to amide III (mainly attributed to the N−H bending vibrations of the peptide amide) are not observed in the spectra for the Rh*−peptide complex (b). Amide II bands at 1555 (+), 1537 (−), and 1523/1514 (+) cm^{-1} in the spectrum for Gt complex formation (a) are replaced by bands at 1551 (+), 1529 (−), and 1510 (+) cm^{-1} with slight downshifts upon Rh*−peptide complex formation (b).

We next tried to detect possible participation of the peptide amide of two crucial apolar residues, Leu344 and Leu349 (*5*, *6*). The same protocol was applied to the peptides with the same sequence, but the peptide amide N−H of either

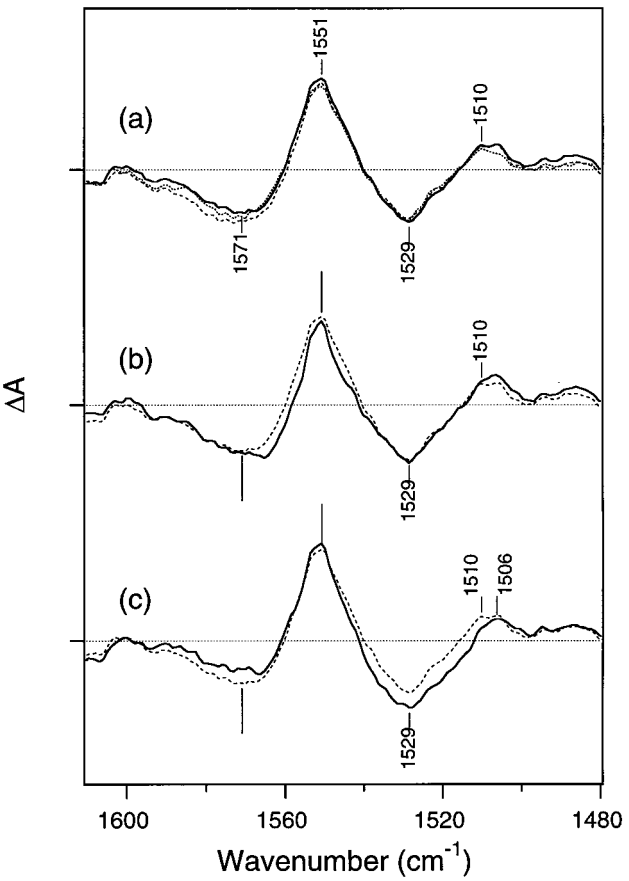

FIGURE 7: The difference FTIR spectra for before and after formation of the complex in the region of 1610−1480 cm^{-1}. The difference spectra for the 20 (a, thick solid line) and 10 (a, dotted and broken lines) samples of the parent peptide are overlaid to show the reproducibility. The difference spectra for the L344 ^{15}N-labeled peptide (b, thick solid line) and the L349 ^{15}N-labeled peptide (c, thick solid line) are overlaid with that for the parent peptide (broken lines in b and c). One division of the ordinate is 0.002 absorbance unit.

Leu344 or Leu349 was labeled with ^{15}N. The reaction with these labeled peptides proceeds exactly in the same way in terms of the quantitative kinetic constant and in its final extent (not shown). In Figure 6 the spectra for these labeled peptides (c and d, respectively) are compared with that for the unlabeled parent peptide (b). The shape of the spectra with the labeled peptides is almost indistinguishable from that of the unlabeled peptide.

Changes in the Peptide Amide of Leu349. If these amide bands are due to the peptide amides of Leu344 and Leu349, they would be detected by an isotope shift in frequency of the amide II vibrations by labeling either of these peptide amides with ^{15}N. The expected isotope shift (labeled minus unlabeled) for this mode is −4 to −12 cm^{-1} (*29*). Though shifts in the major bands were not detected in the spectra in Figure 6 with the labeled peptides, closer inspection of expanded spectra in the 1620−1480 cm^{-1} region in Figure 7 reveals a reproducible shift.

The difference spectrum for all 20 samples of the parent peptide is shown in (a) by a solid line. The duplicated spectra for each 10 samples randomly divided from the 20 spectra (dotted and broken lines) are overlaid. These are largely conincident with each other, showing the reproducibility of the spectra except for slight deviations in the region of 1580−1560 cm^{-1}. The spectra with the ^{15}N-labeled peptides for Leu344 and Leu349 (solid lines in b and c, respectively) are overlaid with the spectral shape for the unlabeled peptide with the spectrum for the 20 samples of (a) by dotted lines. Incorporation of ^{15}N label in the peptide amide of Leu344 does not cause frequency shifts (b). On the other hand, a clear 4-cm^{-1} isotope shift of a positive band at 1510 cm^{-1} due to the Rh*−peptide complex is observed only by the incorporation of ^{15}N label in the peptide amide of Leu349 (c). The corresponding isotope shift of bands due to the mixture of Rh* and the peptide before formation of the complex does not appear clearly; there is a discrepancy between the unlabeled and labeled spectra in the negative band in the region of 1540−1515 cm^{-1}, especially a feature which shows a lower frequency shift at 1530−1515 cm^{-1} only for the label in the peptide amide of Leu349 and seems to contain a corresponding shift. We conclude that the amide II vibration of L349 undergoes frequency change from this region toward 1510 cm^{-1} upon complex formation.

DISCUSSION

The formation of a complex with the 11-mer peptide is accompanied by the appearance of a 1750-cm^{-1} band due to the perturbation of intramembrane carboxylic acid residues Asp83 and Glu122 (*30*). This occurs with a concomitant depletion of the 951-cm^{-1} band due to the twisting of the retinal side chain (*31*). The process for the complex formation is not simple. The deprotonation of the Schiff base occurs later than the formation of the MII-like structure, as envisaged by the appearance of several protein changes as well as the disappearance of the characteristic HOOP band of MI. The complex first appears with the protonated Schiff base with the accompanying transient formation of an α-helix, perhaps at the site for the direct interaction (Figure 4a). It then rapidly converts to a transient state (Figure 4b,c) while keeping the protonated Schiff base (Figure 1, closed circles). The stable complex with the unprotonated Schiff base is preceded by the second transient state with the protonated Shiff base. Both exhibit the identical FTIR spectral shape (Figure 4c,d), irrespective of the protonated states of the Schiff base. Such a complex with the protonated Schiff base was not observed in the previous study for the complex with transducin (*18*). The complex with the protonated Schiff base is also produced in the MII-like species by an E113A/A117E mutant protein (*32*). This mutant protein can stimulate the binding of GTP to Gt upon photo reaction (*33*). Recently, Tachibanaki et al. (*23*, *24*) identified an intermediate in the activating process of both chicken and bovine rhodopsin that binds to Gt but does not facilitate guanine nucleotide exchange in Gt. This intermediate, named Meta Ib, has a protonated Schiff base as judged from the visible spectrum. Thus, the Meta Ib with the protonated Schiff base must be interacting with a localized site in Gt, for example, in the C-terminal region, but without exerting any further changes in the nucleotide binding. Conversely, the lack of the functional linkage to the nucleotide binding site might stabilize the protonated Schiff base in the interaction with the peptide.

Difference FTIR spectra upon formation of the Rh*−Gt complex reveal several changes in hydrogen bonds (*18*). The use of the C-terminal 11-mer peptide, which mimics the most

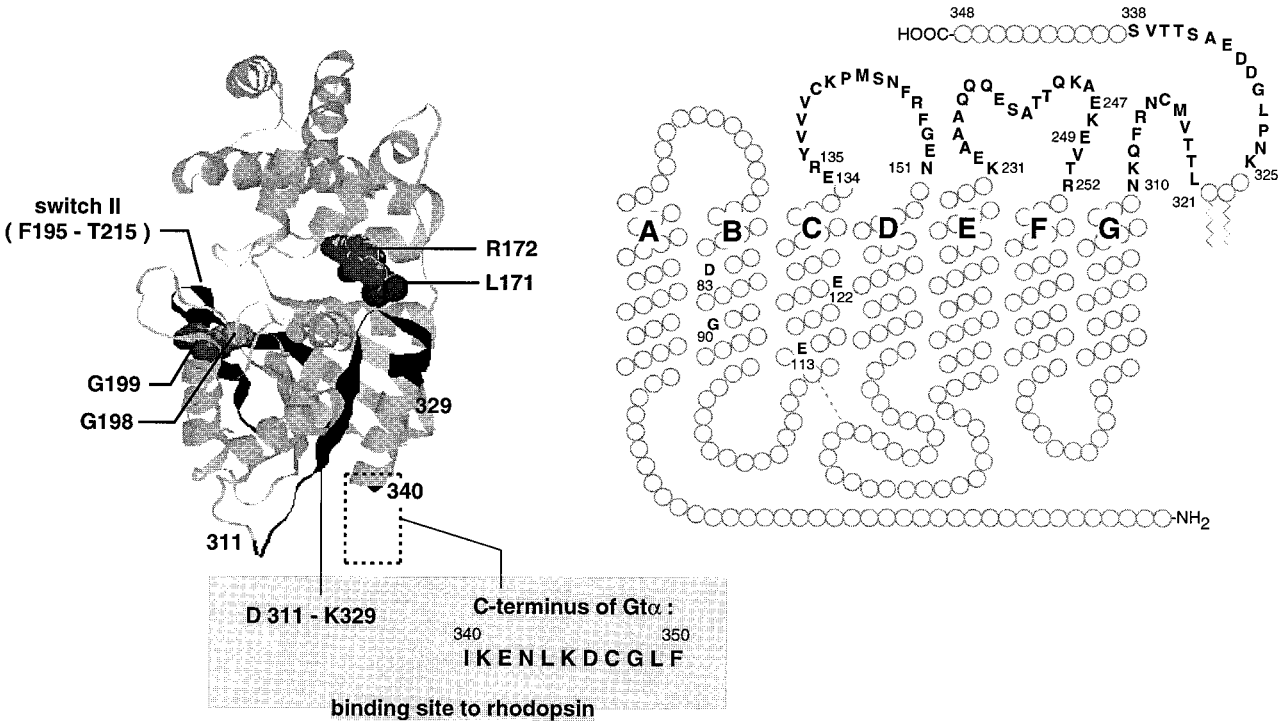

FIGURE 8: Location of residues in transducin and rhodopsin cited in this manuscript. Transducin is depicted on the basis of the coordinates by Lambright et al. (ref 11). The binding site of transducin in rhodopsin is shown according to König et al. (ref 39) and Phillip and Cerione (ref 43).

prominent binding site in Gtα, enables us to discriminate the changes in the sites for the direct interaction between the C-terminal region of Gtα with Rh* from remote sites in rhodopsin or Gt. The overall features of rhodopsin and Gtα are shown in Figure 8. The changes that are observed in the spectrum for the formation of the Rh*−Gt complex but not in the spectrum for the formation of the Rh*−peptide complex can be assigned to those in another weaker binding site of Gt (for example, residues 311−328 in Gtα) (*2*) and sites for the binding of GDP, which is released in the complex.

The C═O stretch bilobe bands of the protonated carboxylic acid at 1770 (−) and 1760 (+) cm^{-1} could not be ascribed to Asp83 or Glu122 of rhodopsin, because these residues exhibit the bands around 1750 cm^{-1} in MII (*30*). The presence of a similar band in the absolute spectrum of the peptide support a notion that either Glu342 or Asp346 is a candidate. Rh−Glu247 and Rh−Glu249 in loop EF of rhodopsin (*34*) may also be candidates. Rh−Glu134, which is in the boundary between helix C of rhodopsin and the cytoplasm, mediates light-dependent proton uptake by MII (*35*) and constitutes the site with Rh−Arg135 that directly provides the signal from rhodopsin to Gt (*36*). However, it is still uncertain whether Rh−Glu134 is in a protonated state in MII. A high-frequency C═O stretching vibration at 1770 cm^{-1} must be due to the carboxylic acid in a quite apolar environment (*37*) and may be present in a hydrophobic pocket of the interaction surface. The negative band at 1713 cm^{-1} in the spectrum for the formation of the peptide complex could be due to the deprotonation of the protonated carboxylic acid. This frequency is identical to that of the protonated Rh−Glu113 (*32*).

Strengthening of the hydrogen bonds of peptide carbonyls observed upon Rh*−Gt complex formation, which appear as amide I bands at 1674 (−), 1661 (−), and 1640 (+) cm^{-1}, is absent in the reaction with the peptide. Thus, these changes of the peptide carbonyls possibly occur in another site of Gtα associated with the binding of GDP, which releases from it upon complex formation. The peptide carbonyls of Gtα−Leu171 and −Arg172 are shown to bind to the sugar moiety of ribose 2′ and 3′ groups (*10*). These must be changed upon GDP release. The exchange for GDP by GTP may also result in a hydrogen bonding change in the peptide carbonyls of Gtα−Gly198 and −Gly199 in the switch II region (Gtα 195−215). Corresponding possible changes are detected as the bilobe with a negative band at 1664 cm^{-1} and a positive band at 1653 cm^{-1} in our previous study (Figure 2d in ref 18). This negative band at 1664 cm^{-1} might also be changed in the complex formation with Gt, but this is hard to observe due to the overlapped bands (Figure 4c in ref 18).

The 1687-cm^{-1} band is conserved in the spectrum for the complex formation with the 11-mer peptide. It is hard to imagine that this could result from the perturbation of the peptide carbonyl of Gly90 of rhodopsin (*38*). The positive band at 1657 cm^{-1} could be associated with strengthening of the hydrogen bond of the mode for the 1687-cm^{-1} band and/or intensification of the vibrational modes of the 1657-cm^{-1} band by environment changes. These could be ascribed to the formation of an α-helix in the 11-mer peptide of Gtα. Kisselev et al. (*16*) pointed out that the N-terminal part of the 11-mer peptide tends to form an α-helix upon binding to MII. Alternatively, these changes occur at a part of three cytoplasmic loops and a part of the C-terminal tail of rhodopsin (*39*) that contributes to the binding and activating of Gt but not to interaction with the C-terminal region. Residues between Rh−Gln237 and −Ala246 in the EF loop (*34, 40, 41*) satisfy these requirements.

Hydrogen bonds of a few peptide amides which are involved in the binding to α and β phosphate oxygens (*10*) would be lost upon complex formation. These could comprise the amide III bands which appear in the complex formation with Gt but are absent in the complex formation with the peptide. It is not certain whether corresponding amide II bands, which would be present in the spectrum for the complex formation with Gt, are lost in the spectrum for the formation of the complex with the peptide. The latter spectrum apparently exhibits the bands which show shifts from the former.

The amide II band due to Leu349 shifts from the region of 1530−1515 cm^{-1} toward 1510 cm^{-1} upon complex formation. These frequencies of amide II are extremely low for amide II. Amide II vibration is a coupled mode of two vibrational modes of a peptide bond, C−N stretching and N−H bending vibrations. Low frequency of the C−N stretching vibration results from the greater single-bond character of the C−N bond, and the low frequency of the N−H bending vibration results from weak H-bonding. These reflect an extremely apolar and restricted environment around the crucial leucine residue. Distortion around Leu349 upon complex formation may result in more pronounced perturbation of its peptide bond, implying interaction in an apolar environment. This also holds for the structure in the complex deduced by NMR spectroscopy (*16*), in which the N−H of Leu349 points toward the core formed by hydrophobic side chains.

Theoretical considerations by Krimm and Bandekar (*42*) predicted that the third peptide amide among four in a type II′ β-turn exhibits an amide II band around 1520 cm^{-1}. The amide N−H in this structure is at a position not forming a hydrogen bond with the peptide backbone. The γ-turn of some cyclic peptides and rippled pleated β-sheet of polyglycine predicted to contain a 1520-cm^{-1} band cannot be candidates.

This study provides the setup for the detailed analysis of the interaction surface of Rh* with Gt by the further use of labeled peptides and corresponding peptides with replacements of specific residues. Further studies by site-directed mutagenesis and isotope labeling of rhodopsin or Gt will also provide further insights on the molecular mechanism for the interaction inducing the structural changes at the sites for the binding of guanine nucleotide.

Photoactivated rhodopsin not only affects the structure of Gt but also is affected by bound Gt; Gt forces the deprotonation of the Schiff base. The present FTIR study using the C-terminal peptide fragment of Gt reveals variations in the MII-like forms. Further structural analysis of these forms and the use of peptide fragments in other parts may disclose the molecular mechanism connecting the active site of rhodopsin and transducin.

ACKNOWLEDGMENT

S.N. is a recipient of a fellowship from the Japan Society for the Promotion of Science. The authors express their thanks to Prof. Richard Needleman for his help with the grammar.

REFERENCES

1. Neer, E. J. (1995) *Cell 80*, 249−257.
2. Hamm, H. E. (1998) *J. Biol. Chem. 273*, 669−672.
3. Hamm, H. E., Deretic, D., Arendt, A., Hargrave, P. A., König, B., and Hofmann, K. P. (1988) *Science 241*, 832−835.
4. Emeis, D., and Hofmann, K. P. (1981) *FEBS Lett. 136*, 201−207.
5. Martin, E. L., Rens-Domiano, S., Schatz, P. J., and Hamm, H. E. (1996) *J. Biol. Chem. 271*, 361−366.
6. Osawa, S., and Weiss, E. (1995) *J. Biol. Chem. 270*, 31052−31058.
7. Garcia, P. D., Onrust, R., Bell, S. M., Sakmar, T. P., and Bourne, H. R. (1995) *EMBO J. 14*, 4460−4469.
8. West, R. E., Moss, J., Jr., Vaughan, M., Liu, T., and Liu, T. Y. (1985) *J. Biol. Chem. 260*, 14428−14430.
9. Conklin, B., Farfel, Z., Lustig, K. D., Julius, D., and Bourne, H. R. (1993) *Nature* 363, 274−276.
10. Noel, J. P., Hamm, H. E., and Sigler, P. B. (1993) *Nature 366*, 654−663.
11. Lambright, D. G., Noel, J. P., Hamm, H. E., and Sigler, P. B. (1994) *Nature 369*, 621−628.
12. Sondeck, J., Lambright, D. G., Noel, J. P., Hamm, H. E., and Sigler, P. B. (1994) *Nature 372*, 276−279.
13. Lambright, D. G., Sondek, J., Bohm, A., Skiba, N. P., Hamm, H. E., and Sigler, P. B. (1996) *Nature 379*, 311−319.
14. Dratz, E. A., Furstenau, J. E., Lambert, C. G., Thireault, D. L., Rarick, H., Schepers, T., Pakhlevaniants, S., and Hamm, H. E. (1993) *Nature 363*, 276−281.
15. Dratz, E. A., Furstenau, J. E., Lambert, C. G., Thireault, D. L., Rarick, H., Schepers, T., Pakhlevaniants, S., and Hamm, H. E. (1997) *Nature 390*, 424.
16. Kisselev, O. G., Kao, J., Ponder, W., Fann, Y. C., Gautam, N., and Marshall, G. R. (1998) *Proc. Natl. Acad. Sci. U.S.A.* 95, 4270−4275.
17. Maeda, A. (1995) *Isr. J. Chem. 35*, 387−400.
18. Nishimura, S., Sasaki, J., Kandori, H., Matsuda, T., Fukada, Y., and Maeda, A. (1996) *Biochemistry 35*, 13267−13271.
19. Yamazaki, Y., Tuzi, S., Saitô, H., Kandori, H., Needleman, R., Lanyi, J. K., and Maeda, A. (1996) *Biochemistry 35*, 4063−4068.
20. Yamazaki, Y., Kandori, H., Needleman, R., Lanyi, J. K., and Maeda, A. (1998) *Biochemistry 37*, 1559−1564.
21. Nagata, T., Terakita, A., Kandori, H., Kojima, D., Shichida, Y., and Maeda, A. (1997) *Biochemistry 36*, 6164−6170.
22. Stern, L. J., Brown, J. H., Jardetzky, T. S., Gorga, J. C., Urban, R. G., Strominger, J. L., and Wiley, D. C. (1994) *Nature 368*, 215−221.
23. Tachibanaki, S., Imai, H., Mizukami, T., Okada, T., Imamoto, Y., Matsuda, T., Fukada, Y., Terakita, A., and Shichida, Y. (1997) *Biochemistry 36*, 14173−14180.
24. Tachibanaki, S., Imai, H., Terakita, A., and Shichda, Y. (1998) *FEBS Lett. 425*, 126−130.
25. Kandori, H., and Maeda, A. (1995) *Biochemistry 34*, 14220−14229.
26. Lowry, O. H., Rosenbrough, N. J., Farr, A. L., and Randall, R. J. (1951) *J. Biol. Chem. 193*, 265−275.
27. Maeda, A., Ohkita, Y. J., Sasaki, J., Shichida, Y., and Yoshizawa, T. (1993) *Biochemistry 32*, 12033−12038.
28. Sasaki, J., Yuzawa, T., Kandori, H., Maeda, A., and Hamaguchi, H. (1995) *Biophys. J. 68*, 2073−2080.
29. Bandekar, J., and Krimm, S. (1985) *Int. J. Pept. Protein Res. 26*, 407−415.
30. Fahmy, K., Jager, F., Beck., M., Zvyaga, T. A., Sakmar, T. P., and Siebert, F. (1993) *Proc. Natl. Acad. Sci. U.S.A.* 90, 10206−10210.
31. Ohkita, Y. J., Sasaki, J., Maeda, A., Yoshizawa, T., Groesbeek, M., Verdegem, P., and Lugtenburg, J. (1995) *Biophys. Chem. 56*, 71−78.
32. Fahmy, K., Siebert, F., and Sakmar, T. P. (1994) *Biochemistry 33*, 13700−13705.
33. Zvyaga, T. A., Fahmy, K., and Sakmar, T. P. (1994) *Biochemistry 33*, 9753−9761.
34. Acharya, S., Saad, Y., and Karnik, S. S. (1997) *J. Biol. Chem. 270*, 6519−6524.
35. Arnis, S., Fahmy, K., Hofmann, K. P., and Sakmar, T. P. (1994) *J. Biol. Chem. 269*, 23879−23881.

36. Acharya, S., and Karnik, S. S. (1996) *J. Biol. Chem. 271*, 25406−25411.
37. Dioumaev, A. K., and Braiman, M. S. (1995) *J. Am. Chem. Soc. 117*, 10572−10574.
38. Zvyaga, T. A., Fahmy, K., Siebert, F., and Sakmar, T. P. (1996) *Biochemistry 35*, 7536−7545.
39. König, B., Arendt, A., McDowell, J. H., Kahlert, M., Hargrave, P. A., and Hofmann, K. P. (1989) *Proc. Natl. Acad. Sci. U.S.A.* 86, 6878−6882.
40. Franke, R. R., Sakmar, T. P., Graham, R. M., and Khorana, H. G. (1992) *J. Biol. Chem. 267*, 14767−14774.
41. Ernst, O. P., Hofmann, K. P., and Sakmar, T. P. (1995) *J. Biol. Chem. 270*, 10580−10586.
42. Krimm, S., and Bandekar, J. (1980) *Biopolymers 19*, 1−29.
43. Phillips, W. J., and Cerione, R. A. (1994) *Biochem. J. 299*, 351−357.

BI981451N